INTERPRETATION OF BIOMEMBRANE STRUCTURE BY RAMAN DIFFERENCE SPECTROSCOPY

NATURE OF THE ENDOTHERMIC TRANSITIONS IN PHOSPHATIDYLCHOLINES

BRUCE P. GABER, PAUL YAGER, AND WARNER L. PETICOLAS,
Department of Chemistry, University of Oregon, Eugene, Oregon 97403 U. S. A.

ABSTRACT Raman difference spectroscopy has been applied to aqueous dispersions of dipalmitoyl phosphatidylcholine (DPPC). Difference spectra have been created by computer subtraction of absolute Raman spectra taken in each of three different temperature ranges: below the endothermic pretransition at 34 ± 2°C; between this temperature and the melting transition at 42°C; and above the melting temperature. The resultant difference spectra are both quantitatively and qualitatively different, indicating that a distinct phospholipid conformation occurs in each of the three temperature ranges. Furthermore, the difference spectra show details of Raman spectral changes with greater clarity than is possible with conventional Raman techniques. A description of the lateral interchain order and the longitudinal chain order is given for each of the three temperature ranges. In addition to obtaining a more precise quantitative measurement of the changes in the Raman spectra, we observed some significant and previously unreported changes. It is suggested that distortion in the hexagonal lattice below the pretransition temperature previously reported by X-ray diffraction techniques may be responsible for interchain interactions which give rise to a Raman band observed only in the triclinic lattice of even-numbered *n*-alkanes.

INTRODUCTION

This laboratory recently reported Raman melting curves for dipalmitoyl phosphatidylcholine (DPPC)[1] dispersions in which abrupt changes in the Raman spectra were observed at temperatures corresponding to the endothermic melting (i.e., gel-to-liquid crystal) transition at 42°C as well as to the pretransition at 34 ± 2°C (1). Our preliminary interpretation of these data included the conclusion that the premelt is characterized by a pronounced change in the lateral interaction between the hydrocarbon chains, while the melt is marked by a substantial increase in the number of *gauche* rota-

[1] *Abbreviations used in this paper:* DPPC, 1,2-dipalmitoyl phosphatidylcholine; T_m, gel-liquid crystal transition temperature; T_{pre}, "pretransition" temperature.

Dr. Gaber's current address is: Department of Biochemistry, School of Medicine, University of Virginia, Charlottesville, Va. 22901, and Optical Techniques Branch, Naval Research Laboratory, Washington, D.C. 20375.

tions about the C—C bonds. In this paper we extend our earlier ideas with results obtained by a differential Raman technique, allowing identification of three distinct bilayer conformations of DPPC. We offer further clarification of the conformation of these bilayer structures in terms of intra- and interchain conformation in three separate ranges of temperatures: below T_{pre}, between T_{pre} and T_m, and above T_m.

METHODS

Samples of the L-isomer of DPPC were purchased from various suppliers (Calbiochem, San Diego, Calif., and Sigma Chemical Co., St. Louis, Mo.) and routinely purified by chromatography on a column of Sephadex LH-20 (ethanol, 37°C). Hexadecane was obtained from Applied Science Labs, Inc., State College, Pa., hexadecane-d_{34} from Merck, Sharpe and Dohme, (Merck & Co., Inc., Rahway, N. J.) and heptadecane from Aldrich Chemical Co., Inc., Milwaukee, Wis. Lipid purity was determined by differential scanning calorimetry of dilute aqueous dispersions of the lipid in a calorimeter of the Privalov design (2), model DASM-1M, constructed by the Academy of Sciences, USSR, Scientific Institute, Department for Biological Instrumentation.

Phospholipid dispersions were prepared for Raman measurements as follows. About 1.0 mg of dry phospholipid was weighed into a melting point capillary and 10 μl of buffer (0.01 M Tris, pH 8, 0.1 M KCl) added, giving a concentration of 100 μg/μl. After the capillary was sealed, the sample was heated to 50°C, briefly homogenized in a low-power bath sonicator, and centrifuged to the bottom of the capillary. This procedure was repeated at least three times. Such samples were saturated with respect to the aqueous phase (3) and, being highly dispersed, were turbid at all temperatures studied. When samples were prepared by allowing the lipid to swell without agitation, large birefringent transparent domains were created. Such samples demonstrate changes in overall Raman scattering intensity with temperature, whereas the dispersed turbid preparations used in our Raman experiment did not.

Raman spectra were obtained with a system consisting of a Spex 1301 double monochromator (Spex Industries, Inc., Metuchen, N.J.), a Spectra-Physics model 165 argon ion laser (Spectra-Physics Inc., Laser Products Div., Mountain View, Calif.), photon-counting electronics with a counter attached to a Varian 620/i computer (Varian Associates, Palo Alto, Calif.), and a sample holder thermostated to ±0.2°C. All spectra were taken in order of ascending temperature. Samples were annealed for at least 1 h at the lowest measuring temperature. In no case was the temperature taken below −14°C. Temperatures were corrected by +2.6°C to account for laser heating. Spectral slit widths were 3–4 cm^{-1} for the phospholipid samples and 2–3 cm^{-1} for the hydrocarbon samples.[2] The 5,145 Å line of the laser was used for excitation.

The computer was programmed to step the wavenumber drive 1 cm^{-1}/s, counting and storing photoelectron pulses during the 1-s interval. By taking several scans and adding the counts at each wave number, it was possible to obtain a higher signal-to-noise Raman spectrum than with a conventional Raman spectrograph. Base lines were subtracted for convenience of display and spectra so noted in figure captions were smoothed by the method of Savitsky and Golay (4).

The method for producing presentable data with computerized techniques is sufficiently different from the methods employed in conventional Raman spectroscopy to merit mention. In the standard technique one eliminates the high-frequency noise fluctuations in signal intensity inherent to Raman scattering experiments by introducing a resistance-capacitance (RC) time constant into the electronic circuitry to give an exponential damping before final transference

[2]At 5145°A reciprocal dispersion of the monochromator is 0.028 $cm^{-1}/\mu m$ at 1,000 cm^{-1} Stokes shift and 0.021 $cm^{-1}/\mu m$ at 3,000 cm^{-1}.

of the Raman signal to a strip chart recorder. By slowing the scanning rate and utilizing a long time constant, one can produce aesthetically pleasing spectra, but the RC circuit may introduce some asymmetry into the Raman bands, converting the high-frequency noise into low-frequency, highly convoluted noise in the spectra. Low-frequency noise is also inherent in the Raman measurement because of slowly varying long-term fluctuations in the sample or laser. Since this slowly varying noise component is not removed by the RC filter, substantial differences in relative peak intensities may occur between successive single scans of the sample. Digital manipulation of the data is also subject to noise problems, but these can be dealt with in a more straightforward manner. Averaging of many spectra reduces both high and low frequency noise to acceptable levels. But when the time involved for production of completely smooth spectra is prohibitive, digital smoothing techniques, such as the method of Savitsky and Golay (4), can be employed which do not skew the data systematically in one direction, and preserve both peak intensities and shapes.

Subtraction of two spectra with finite signal-to-noise levels results in a difference spectrum with a signal-to-noise level inferior to that of the two absolute spectra, since the signals are subtracted and the noise added. However, with Raman difference data there are few possible sources for error. A lack of reproducibility in absolute positions of bands can arise from backlash or long-term drift in the monochromator wavelength drive. Such difficulties are usually alleviated by repeated scanning of samples. However, any such artifacts are readily identified as difference spectra which show the same apparent frequency shift for all Raman bands. Drift in laser power, sample scattering efficiency, or background luminescence may also result in spurious differences. Our laser is stable in light output, and all of these difficulties are greatly minimized by averaging many spectra. Each scan can be displayed on an oscilloscope so that transient phenomena, such as bubbles in the sample, that produce sharp spikes in the spectrum are easily identified, and such spectra may be eliminated from the averaged scans. To avoid artificial band-broadening and band-narrowing effects, the data must be collected so that the spectral bandwidth remains the same, point-for-point, for any two spectra being compared (i.e. the slit widths must be the same for all spectra). For further discussion of the advantages of Raman difference spectroscopy, see ref. 5.

In our experiments difference spectra have been created by subtracting spectra taken at high temperatures from those taken earlier with the same number of scans on the same sample in the same position at lower temperatures. Thus, if a band loses intensity as the sample is heated, the loss appears as a positive peak in the difference spectrum, and if a band gains intensity at the higher temperature, the gain appears as a negative peak. More complex changes, such as shifts in frequency and changes in bandshapes, will be discussed below. However, only perturbed bands, i.e., Raman bands which change intensity, frequency, or width with changing temperature in the sample, are observed in the difference spectra. Consequently, the difference spectra are simplified relative to the absolute spectra from which they are derived, since the temperature-invariant bands are missing. Thus all temperature-invariant bands act effectively as internal standards.

RESULTS AND DISCUSSION

Figs. 1 and 2 show Raman spectra of a DPPC dispersion at temperatures characteristic of the three regions of the phase behavior, with an additional spectrum in Fig. 2 substantially below T_{pre}. As was shown previously by Gaber and Peticolas (1), there is a gradual change in the Raman spectrum of DPPC with temperature throughout the range 15–50°C, with abrupt changes at the two transition temperatures, T_{pre} and T_m.

As can be seen from Fig. 1, the intensity of the C—N stretch appears to remain unchanged throughout the whole temperature range. If one excludes the unlikely co-

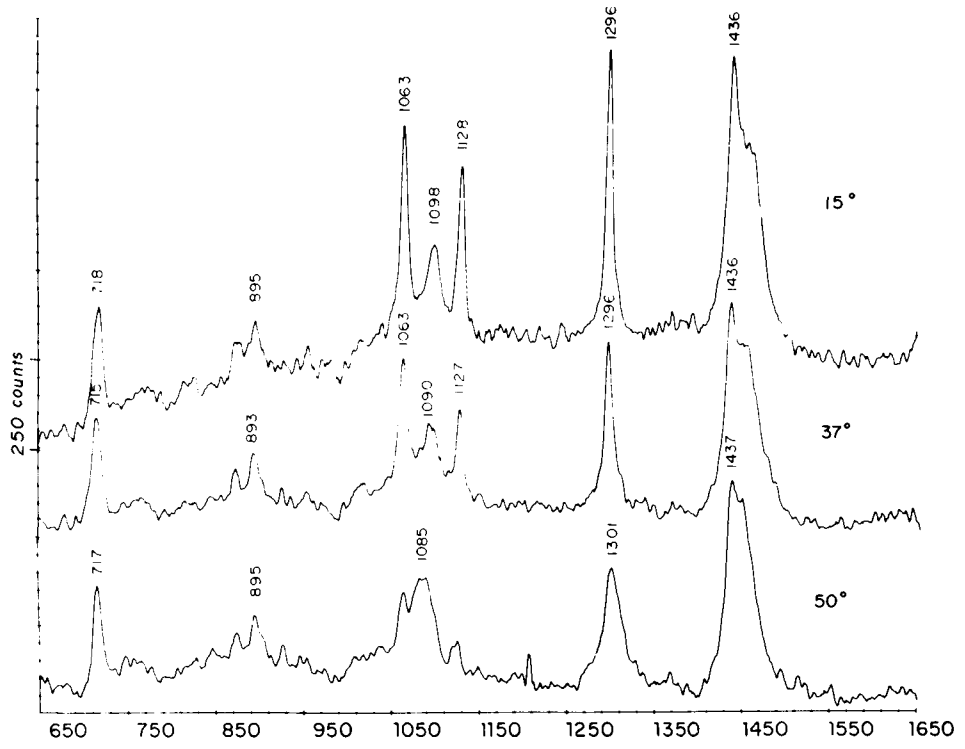

FIGURE 1 Raman spectra of a DPPC dispersion at 15°, 37°, and 50°C. The x axis is in units of change in reciprocal centimeters, and all three spectra are shown on the same scale. Each spectrum represents an average of 10 scans with the laser at 300 mW of 5,145 Å radiation, and 200 μm slit width. These spectra have been nine-point smoothed.

incidence that a phase transition simultaneously alters the overall scattering intensity of the phospholipids but changes the relative height of the C—N stretching band in an equal but opposite sense, then the use of this band as an intensity standard in previous work by several laboratories (1, 6) would seem justified.

From a simple visual inspection of Figs. 1 and 2 one can see the well-known changes in the skeletal optical modes at 1,064 cm^{-1} and 1,128 cm^{-1} (1, 7–9), as well as changes in the CH_2 stretching manifold (1, 6, 10–14). The skeletal optical modes, being essentially C—C stretches delocalized along the entire acyl chain, provide information on intrachain conformations. The CH_2 stretches, on the other hand, are not strongly coupled to the chain, but are particularly sensitive to interchain or lateral interactions in the bilayer. Detailed interpretation of these spectral regions in terms of intra- and interchain effects follows the discussion of the data.

Differences between the Raman spectra in each of the three temperature regions are best demonstrated by the Raman difference spectra (Figs. 3 and 4) obtained by simple subtraction of the unnormalized data in Figs. 1 and 2.

The C—N stretch at 718 cm^{-1} is constant and does not appear in the difference

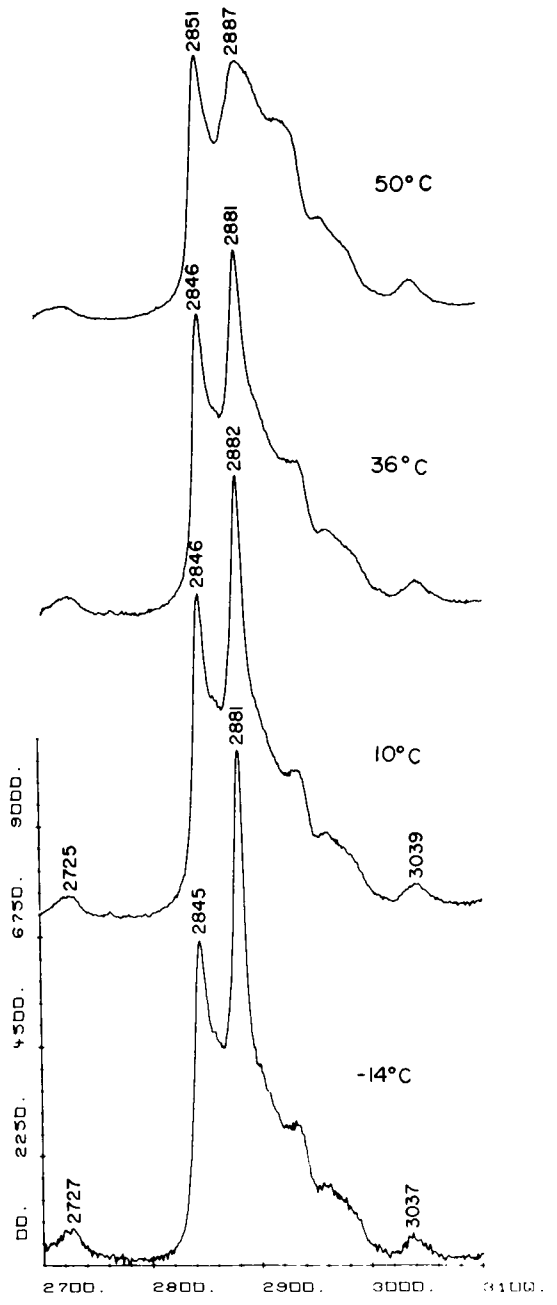

FIGURE 2 Raman spectra in the CH_2 stretching of a DPPC dispersion at −14°, 10°, 36°, and 50°C. All four spectra are shown on the same scale. Slits were set at 150 μm, and 400 mW of 5,145 Å radiation was used. Spectra are shown unsmoothed, and are averaged from 15 scans.

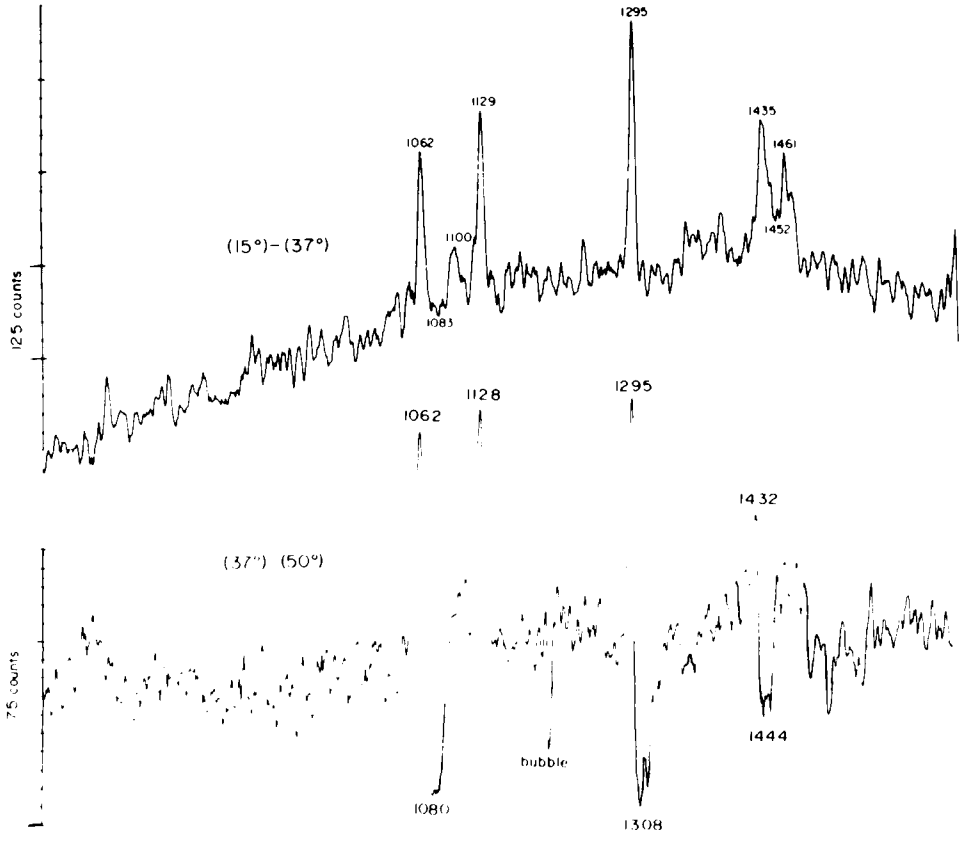

FIGURE 3 Difference spectra created by computer subtraction of the data shown in Fig. 1. The peak marked "bubble" results from a noise peak in the 50°C spectrum in Fig. 1.

spectra. Fig. 3 also shows no differences above the noise level in the region from 800 to 1,000 cm^{-1}. A detailed list of all significant changes with their assignments is given in Table I.

Evidence for Three Distinct Bilayer Structures

If we take the Raman spectrum at 15°C as characteristic of the ordered structure existing in the DPPC dispersion below T_{pre}, then Figs. 3 and 4 show that the degree of order at 37°C, between the two transition temperatures, and at 50°C, above T_m, has decreased to different extents.

In the region of the skeletal optical mode (SOM) vibrations, there is a complex set of changes shown in the difference spectra in Fig. 3. The premelt results in losses of intensity at 1,062, 1,100, and 1,129 cm^{-1}. By comparison the melting transition results in a continued intensity decrease for the bands at 1,062 and 1,129 cm^{-1}, superimposed upon which is a strong increase in a broad band centered at 1,080 cm^{-1}. This increase

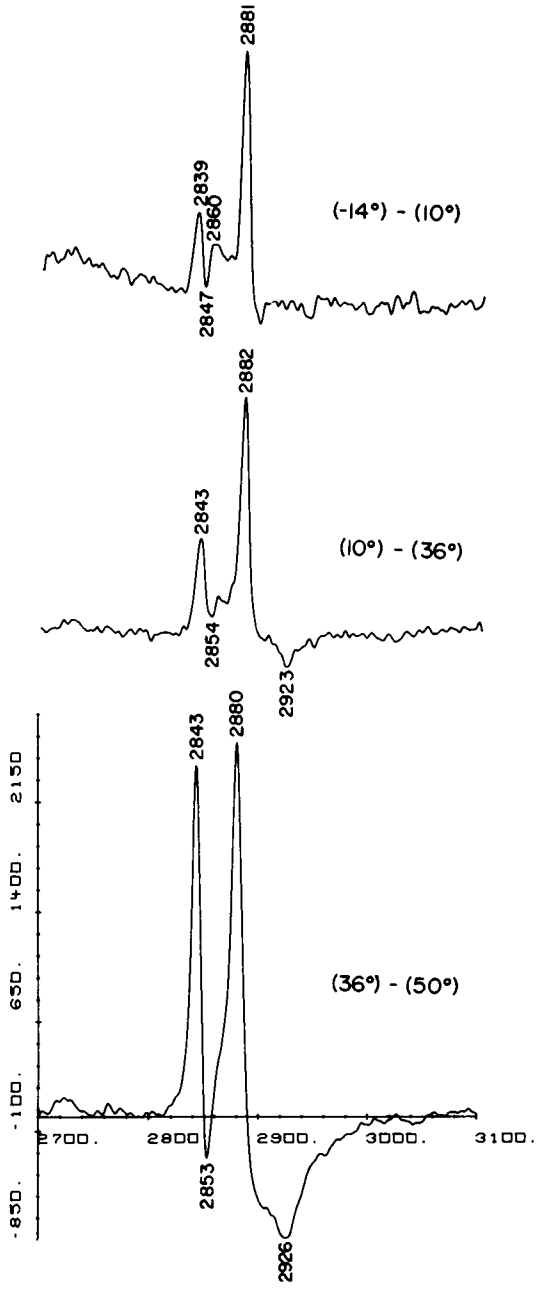

FIGURE 4 Difference spectra created by computer subtraction of data shown in Fig. 2, followed by seven-point smoothing. All spectra are to the same scale.

TABLE I

Assignment	Marker			Δcm^{-1} at 15°	Intensity rel. to 15°	Δcm^{-1} at 37°	Intensity rel. to 15°	Δcm^{-1} at 50°	Intensity rel. to 15°
	Trans	Gauche	Packing						
H_3C—N stretch				718	1.0	715	1.0	717	1.0
SOM	X			1,063	1.0	1,063	0.65	1,063	0.32
SOM *gauche*		X		1,080	1.0	1,070	~1.1	1,085	>5
SOM	X			1,098	1.0	1,090	0.95	?	?overlap with 1,080 cm^{-1}
SOM	X			1,128	1.0	1,127	0.49	1,122	0.04
CH_2 twist		X		1,296	1.0	1,296	0.54	1,301	0.28*
CH_2 sciss			X	1,436	1.0	1,436	0.76	1,439	0.70
CH_2 sym stretch		X	X	2,845	1.0	2,846	0.80	2,850	0.70
CH_2 triclinic marker			X	2,860	1.0	2,860	~0	2,860	~0
CH_2 asym stretch		X	X	2,881	1.0	2,880	0.73	2,888	0.47
CH_2		X		2,920	1.0	2,920	1.0	2,920	1.25 shoulder
CH_3 stretch				2,935	1.0	2,935	1.0	2,935	1.0 shoulder
CH_3 stretch				2,961	1.0	2,961	1.0	2,961	1.0
CH_3 stretch (choline)				3,039	1.0	3,039	1.0	3,039	1.0

SOM, skeletal optical modes.
*Peak broadens.

in the 1,080 cm^{-1} band, upon melting, shows up as a strong negative peak at 1,080 cm^{-1} in the 50°-37°C difference spectrum. A more detailed set of spectra of the skeletal optical region (Fig. 5) show that the band centered at 1,080 cm^{-1} gains intensity only at temperatures near T_m, confirming the conclusion drawn from the difference spectra. Fig. 5 also indicates that as the intensity of the peak at 1,128 cm^{-1} is lost with increasing temperature, the frequency of the band shifts gradually to 1,122 cm^{-1}. This change is too weak to be clearly identified in either Figs. 1 or 3. We never observed this band as a shoulder on the 1,128 cm^{-1} band. A similar band is evident in the spectra of melted fatty acids (8) and in dispersions of racemic DPPC (13).

As may be seen from Figs. 1 and 3, the CH_2 twisting mode at 1,296 cm^{-1} decreases in intensity upon going through the pretransition, while its frequency remains constant. On the other hand, in passing through T_m the behavior of the band is more complex. There is a substantial loss in intensity at 1,295 cm^{-1}. If a Raman band shifts only in frequency and remains constant in intensity and band shape, the resulting difference spectrum will be biphasic, with equal positive and negative lobes with the crossover point midway between the initial and final frequencies. The behavior of the CH_2 twisting band in the 37°-50°C difference spectrum shows that the band not only shifts in frequency but also broadens considerably, thus destroying the symmetry of the differential spectrum. (See also ref. 9.)

The difference spectra of the CH_2 scissor modes indicate losses of intensity at 1,435

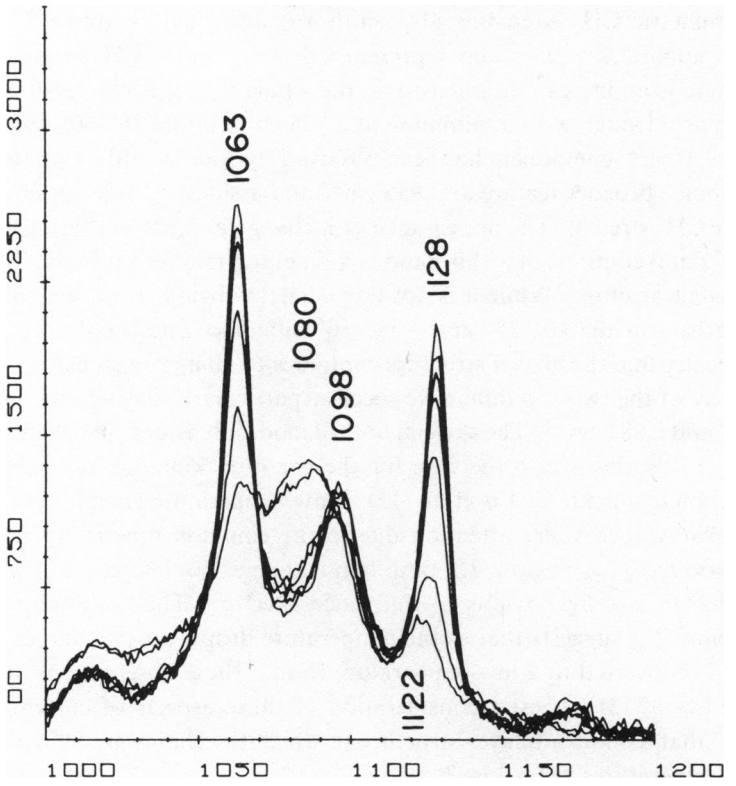

FIGURE 5 A superposition of seven spectra of the skeletal optical mode region of a DPPC dispersion taken at 15°, 22°, 27°, 32°, 37°, 42°, and 50°C. Each spectrum was taken with 600 mW of 5145 Å light, with 200 μm slit width, with six scans averaged. All base lines were set to zero but no smoothing or normalization has been performed. Throughout the temperature region the peak at 1,063 cm^{-1} decreases in intensity, as does that at 1,128 cm^{-1} with a shift to lower Δ cm^{-1}. The peak at 1,098 cm^{-1} appears to decrease slightly at T_{pre}, whereas the peak centered at 1,080 cm^{-1} only increases at 42°C and above.

and 1,460 cm^{-1} upon premelting, whereas upon melting there is an actual increase at 1,444 cm^{-1} that corresponds to the narrowing of the whole band complex (Fig. 1).

The Raman difference spectra of the C—H stretching region (Fig. 4) provide further evidence for the existence of three distinct bilayer structures. From 10° to 36° (just above the pretransition) both the 2,882 and 2,843 cm^{-1} methylene stretches decrease in intensity, with the former undergoing almost twice the change of the latter. We also find a positive peak in 10°–36° difference spectrum at 2,850 cm^{-1}. This is evidently a Raman band present in the 10°C spectrum but missing in the 36°C spectrum. Its significance will be discussed below. A small increase in intensity occurs at 2,923 cm^{-1}. By contrast, upon melting, while there are very large intensity decreases at 2,843 and 2,880 cm^{-1}, the relative changes in the two bands are almost equivalent. By comparison with the spectra shown in Fig. 2, we conclude that the origin of the dip at 2,853 cm^{-1} in Fig. 4 is the result of the frequency shift of the CH_2 symmetric stretch.

The asymmetric CH_2 stretching also shifts (to 2,888 cm^{-1}) above T_m. A small shoulder at about 2,871 cm^{-1} may represent a decrease in the CH_3 symmetric stretch. At 50°C there is an increase in intensity in the whole region 2,890–2,940 cm^{-1}, which can be seen as a trough with a minimum at 2,926 cm^{-1} in the 36°–50° difference spectrum. A 2,920 cm^{-1} component has been observed by Bunow and Levin (6) as a weak shoulder upon a broader feature at 2,935 cm^{-1} and assigned (14) as an infrared-active asymmetric CH_2 stretch. The appearance of a change at 2,926 cm^{-1} (most notably in the 36°–50° data) confirms that this band is a "melting marker" principally associated with the main transition. While it is not immediately obvious from the absolute spectra, comparison of the 10°–35° and −14°–10° difference spectra (upper two traces, Fig. 4) indicates that the bilayer structure continues to change even below 10°C. Note the similarity of the two top difference spectra, particularly the relative intensities at 2,843 cm^{-1} and 2,881 cm^{-1}. The skeletal optical mode intensities change monotonically below T_{pre} (1, 13); this is also the case for the chain-packing-sensitive CH_2 stretches, an observation first made by Lis et al. (15). Low temperature changes in these modes have perhaps escaped wider attention due to the common practice of reporting the intensity ratio I_{2845}/I_{2880}; below T_{pre} both bands change, but in constant proportion so that the change is only obvious in difference spectra. The continuity of spectral changes below T_{pre} suggests that as the temperature drops, an ever larger fraction of the bilayer is converted to a low-temperature form. These observations and those of Yellin and Levin (13) suggest reconsideration of those aspects of current theoretical models (16) that assume a bilayer structure in which the chains are all *trans* and well-packed at temperatures just below T_m.

Intrachain Conformation

The *trans* conformation of the C—C bonds of the phospholipid hydrocarbon chains are identified in Raman spectra by three bands in the skeletal optical region: two intense ($k = 0$) skeletal stretching modes at 1,129 and 1,062 cm^{-1} may be characterized as "*trans* markers" (1, 7–9). In particular we have argued that the relative intensity of the 1,129 cm^{-1} is related to the number of *trans* bonds per acyl chain (1). However, the band at 1,100 cm^{-1} presents more of an assignment problem. Yellin and Levin (13) have associated this band with *trans* conformations at low temperatures, but an exact assignment was not attempted. We agree and suggest that the 1,100 cm^{-1} band may be the $k = 1$ mode of the skeletal stretch at 1,130 cm^{-1}. The evidence for this assignment comes from several sources. There is a band in solid fatty acids at about 1,100 cm^{-1} that shifts to higher frequencies as the length of the hydrocarbon chain is increased (8). A similar chain-length-dependent band is observed in the infrared at the same frequency, in *n*-alkanes with $N > 10$ (17). A normal coordinate treatment shows that insertion of a single *gauche* rotation at the center of an all-*trans* chain lowers the frequency of this band by approximately 7 cm^{-1} (17). If the assignment of the band at 1,100 cm^{-1} is correct, then its exact frequency might be useful in estimating the average length of all-*trans* segments. However, the 1,100 cm^{-1} *trans* band overlaps with a broad band centered at 1,080 cm^{-1} due to *gauche* rotamers, so that its utility is limited to solid phospholipid samples for which the number of *gauche* bonds is small.

The 1,080 cm^{-1} *gauche* band does not appear to any great extent until above the melting transition. This can be seen in Fig. 3, where the band—in the noise level in the 15°–37° spectrum—has considerable intensity in the 37°–50° spectrum. The asymmetry of this band (see also Fig. 5) indicates that it is a composite of bands centered at and below 1,080 cm^{-1} which arise from a variety of local *gauche*-type conformations. Snyder (17) lists C—C stretching and methylene wagging as the main contributions to the normal coordinate. Furthermore, he suggests that wagging of methylenes of *gauche* bonds adjoining *trans* segments contributes much of the infrared intensity of the band. Both infrared and Raman-allowed vibrations may draw their intensities from the same set of electronic excited states (18). Thus extrapolating from infrared intensity data to the Raman, we might expect that long *trans* segments connected by a single *gauche* bond could result in a broad and quite weak band due to the low concentration of *gauche* bonds. By contrast, methylene wagging modes interacting over very short all-*trans* segments are strongly vibrationally coupled. The result would be a fairly narrow distribution such that most of the band intensity falls near 1,080 cm^{-1}.

With these assignments in mind, we can interpret the difference spectra in Fig. 3. In the 15°–37° difference, the decrease in the bands at 1,062, 1,100, and 1,129 cm^{-1} indicates a loss in the number of *trans* bonds, as previously interpreted (1). On the other hand, absence of the *gauche* Raman band at 1,080 cm^{-1} indicates that when the phospholipid is between the two transition temperatures, the *gauche* bonds occur singly between long *trans* segments, or they are located near the terminal groups of the acyl chain. The number of such *gauche* bonds may be estimated with the order parameter, S_{trans}, introduced previously (1). Using the data in Fig. 3 we estimate that from 15°C to the onset of the pretransition at about 32°C there is a decrease in S_{trans} from 0.85 to 0.75. With our order parameters, this corresponds to an increase of about one *gauche* bond per chain (1).

At the melting temperature there is an increase in the number of *gauche* rotations. This is seen in the 37°–50° difference spectrum as a further decrease in the *trans* markers at 1,062 and 1,128 cm^{-1}, and as a large increase in intensity at 1,080 cm^{-1}. From the argument above that a strong broad band at 1,080 cm^{-1} is due primarily to the appearance of sequences of closely coupled *gauche* bonds, it follows that above the melting point, on average, *trans* segments are shorter.

The frequency shift in the 1,296 cm^{-1} CH_2 twisting mode is also consistent with a melted state conformation that contains a broad distribution of *gauche* rotamers. Conversion of an extended *n*-alkane chain to a nonplanar structure results in the activation of a number of intense infrared wagging modes near 1,300 cm^{-1} (17). Some of these vibrations may enter into resonance with the Raman-active twisting mode, perturbing the Raman band and shifting its frequency slightly.

Interchain Interactions

The packing of the hydrocarbon chains strongly affects their Raman spectra in two particular regions: CH_2 scissoring modes at 1,440 cm^{-1} and the CH_2 stretching modes at twice that frequency, 2,900 cm^{-1}. We have estimated lateral or interchain inter-

actions through analysis of the extent of these relative intensities of the CH_2 stretching bands at about 2,850 and 2,890 cm^{-1} (1).

In the difference spectra (Fig. 4) it is apparent that both the 2,845 and 2,881 cm^{-1} bands of DPPC change in intensity in a complex manner over a wide range of temperatures. These changes are qualitatively different at each of the two transition temperatures, supporting the contention that a distinct conformation exists for the bilayer in each of the three temperature ranges and confirming our previous conclusion (1) that the pretransition involves primarily an alteration in lateral order of the bilayer.

Fig. 4 also shows a decrease in intensity of a band at 2,860 cm^{-1} upon going from 14° to 10°C, and a smaller but similar change through the pretransition temperature. Although this band has not been previously reported in DPPC, close scrutiny of published spectra reveal a band near 2,860 cm^{-1} for solid dilauryl phosphatidylethanolamine. (see ref. 9, Fig. 3).

It is well known (19) that all odd *n*-alkanes with *n* larger than nine undergo a premelting phase transition from an orthorhombic to a hexagonal crystal form about 10°C below their melting points (19). In the alkane phase transition the all-*trans* structure of the hydrocarbon chain is maintained; only the lateral crystalline environment changes. Fig. 6 displays Raman spectra of *n*-heptadecane taken in each of three different temperature regions: below the pretransition, between the pretransition and the melting point, and above the melting point. The pretransition of this hydrocarbon is not an exact model for the pretransition in lipids, but the change in lateral order inherent in the phase transition should have a measurable effect on Raman bands sensitive to lateral order.

Upon premelting there is a change both in the CH_2 stretching and CH_2 scissoring regions, showing that these bands are highly sensitive to changes in the crystal or lateral interaction, whereas *all* other vibrational modes are relatively insensitive. We conclude that the change in the 1,445 cm^{-1} band in DPPC through the premelting range is at least partially due to a change in the packing environment of the hydrocarbon chains. Thus the 1,445 cm^{-1} band may also be monitored along with the CH_2 stretches as a marker of the lateral interaction. Comparison of the CH_2 scissoring bands in the alkane and the lipid (Figs. 1 and 6) show that the lateral environment of the two samples is not the same below their respective pretransitions. But it becomes more nearly the same (i.e. the scissoring Raman bands become more similar) in the region just above their respective pretransitions, where both are in a hexagonal crystalline form.

Raman spectra of even *n*-alkanes in the triclinic form always show a splitting of the symmetric CH_2 stretch into two bands at 2,845 and 2,860 cm^{-1} (10, 20). To prove that the 2,860 cm^{-1} band in hexadecane is due to crystalline interactions, we show Raman spectra of hexadecane in matrices of perdeuterated hexadecane (Fig. 7). Isolation of the hexadecane chains in the triclinic lattice by dilution with deuterated chains results in a drastic relative decrease in intensity of the 2,860 cm^{-1} branch of the vibration. (Note that neither of the crystalline forms of heptadecane has a band at 2,860 cm^{-1} comparable to that in hexadecane.) This band also disappears when all-*trans* hexa-

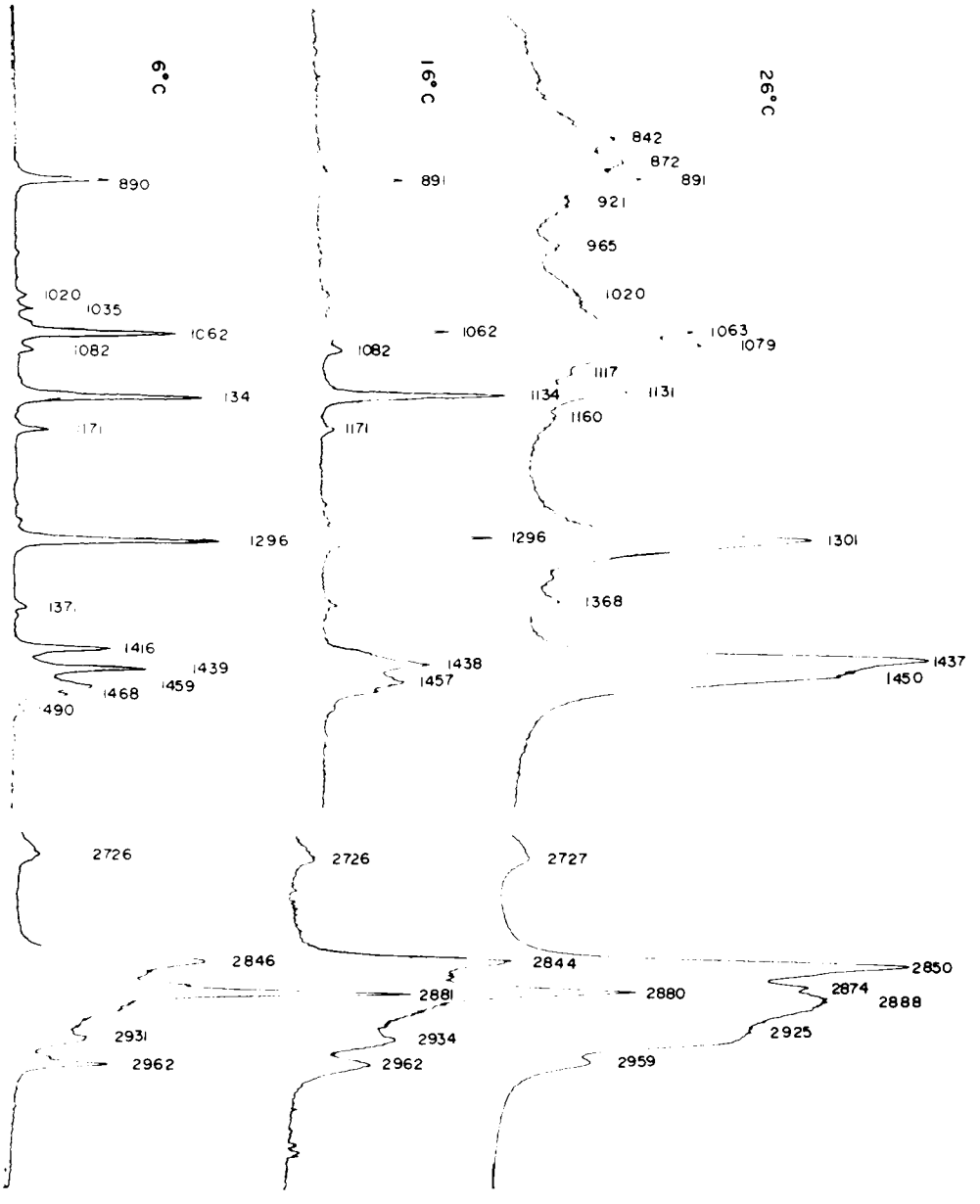

FIGURE 6 Raman spectra of *n*-heptadecane below T_{pre}, between T_{pre} and T_m, and above T_m. Less than 200 mW of 5,145 Å radiation was used in all spectra. The optical properties of the sample were temperature-dependent and intensities of spectra taken at different temperatures should not be compared. Each spectrum represents a single scan with slits set at 100 μm. The longitudinal acoustic mode band was sharp at 140 cm^{-1} at 6°C, sharp at 139 cm^{-1} at 16°C, and broad at 217 cm^{-1} at 26°C. The sample was cooled to just below T_{pre} and annealed for 1 hr before taking spectra in order of ascending temperature.

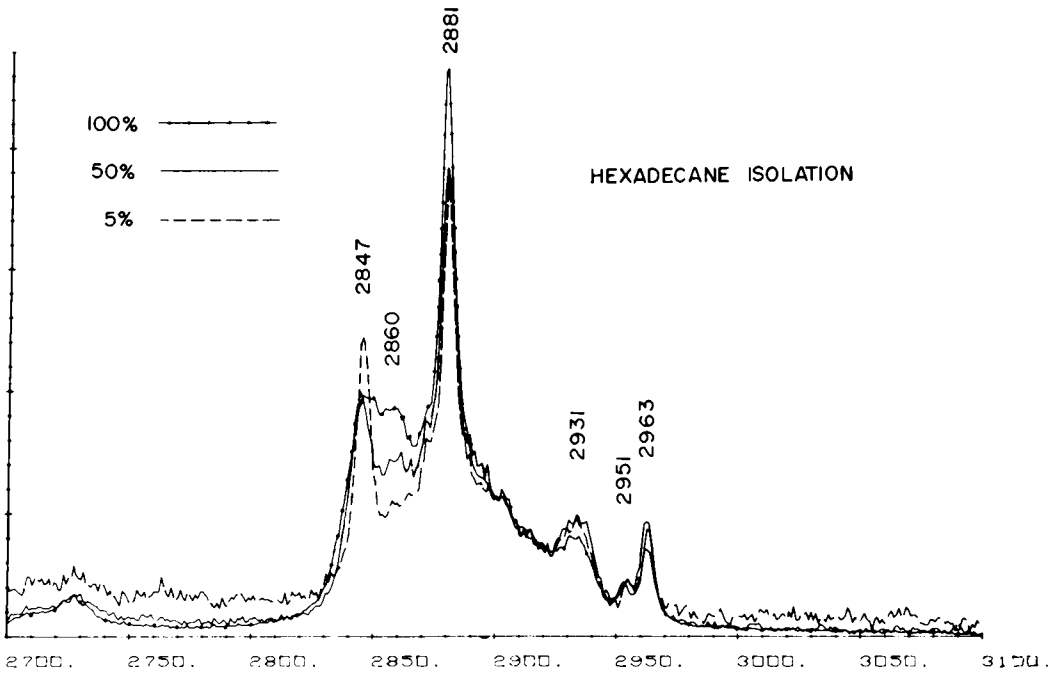

FIGURE 7 Raman spectra of the C—H stretching region of solid solutions of hexadecane in hexadecane-d_{34}. Scaling is arbitrary. The laser excitation was 300 mW of 5,145 Å radiation, with up to 15 scans averaged at 2 cm^{-1} resolution for each spectrum. No smoothing has been employed. Hexadecane-d_{34} has no bands in this region.

decane is isolated in a urea clathrate (Gaber and Peticolas, unpublished results). Thus we assign the 2,860 cm^{-1} band in DPPC below the premelting transition to splitting of the CH_2 symmetric stretch caused by crystalline interactions characteristic of a triclinic lattice. It would seem that in the region between the premelt and the melt the phospholipid chains pack like odd-numbered hydrocarbon crystals, while below the premelt they pack like even-numbered *n*-alkanes.

There are at least two ways in which the hydrocarbon chains in the DPPC bilayer could pack to give rise to a small band at 2,860 cm^{-1}. DPPC bilayers below the premelting transition might consist of patches of triclinically packed phospholipid molecules dispersed in large hexagonally packed domains, with the triclinic domains increasing in size as the temperature is lowered. An alternative hypothesis is more consistent with the "distorted hexagonal lattice" observed by Janiak et al. (21) below the pretransition. The two-dimensional unit cell of the bilayer contains more than one phospholipid molecule, so that within the unit cell there can be several differently oriented fatty acyl chains. Individual pairs of hydrocarbon chains dispersed throughout the lattice might be oriented relative to each other like chains in triclinic crystals, giving rise to "triclinic splitting" of the CH_2 symmetric stretches of those pairs of chains alone. The "distortion" has been observed to increase as the temperature is

lowered (21), and the Raman difference data show that the peak at 2,860 cm^{-1} is more intense at −14°C than at 10°C as the "triclinic distortion" begins to predominate.[3]

CONCLUSIONS

The DPPC bilayer exists in a distinct conformation at each of three well-defined temperature ranges. Each conformation of the bilayer possesses its own characteristic Raman spectrum, the difference between which may be greatly clarified by computer subtraction of the Raman data. The three conformations may be briefly described as follows:

(*a*) Below the pretransition temperature the hydrocarbon chains assume a very nearly all-*trans* conformation and are well packed into a crystalline lattice. The broadening of the CH_2 symmetric stretching band to include a Raman band at 2,860 cm^{-1} below the pretransition temperature is evidence for the existence of lateral chain interactions typical of a triclinic phase. This conclusion is consistent with the X-ray results (21) if it is assumed that the existence of this second phase is responsible for the distortion of the hexagonal phase. A certain degree of freedom of motion for the fatty acyl chains remains below T_{pre}, as there is a gradual increase in the amount of triclinic phase as the temperature is lowered, with a corresponding increase in the intensity of the 2,860 cm^{-1} band.

(*b*) Between the pretransition and the melting temperature the number of *gauche* bonds increases slightly to about one or two *gauche* rotations per chain, giving rise to the well-known intensity changes in the 2,880 cm^{-1} region, as well as newly characterized changes in the 1,445 cm^{-1} range. Our previous conclusion that the primary effect of the pretransition is to reduce the lateral interactions has been confirmed. The absence of the broad strong *gauche* band at 1,080 cm^{-1} is taken as evidence for the absence of *gauche* rotations on adjacent or nearby C—C bonds, indicating that the *gauche* bonds are highly restricted in this phase and are found only at the ends of long all-*trans* segments. Both the absence of the 2,860 cm^{-1} band and the nature of the bands at 1,445 cm^{-1} are consistent with the assumption of a single, loose hexagonal phase and the absence of any triclinic phase.

(*c*) Above the melting transition all of the remaining crystalline chain-chain interaction is lost and the number of *gauche* bonds increases sharply. The appearance of a strong, broad band at 1,080 cm^{-1} indicates that the restriction on the placement of the *gauche* bonds is no longer present in this temperature range; they are free to migrate along the chain to positions on adjacent C—C bonds.

We wish to thank Professor Charles Klopfenstein and Mr. Allen Delwiche of the University of Oregon and Dr. Jean Sturm of the University of Strasbourg for their work on creation and programming of our computerized Raman apparatus, Horst Klump for his aid with the differential scanning calorimetry, and Robert Snyder for stimulating discussion.

[3]It is possible that formation of ice in the sample might influence the state of the bilayer and thereby contribute to intensity in the −14°–10° difference spectrum. However, Ladbrooke and Chapman (22) report that upon cooling, H_2O in lecithin dispersions supercools to at least −15°C. Thus our measurements are made at temperatures at which ice should not be present.

The differential adiabatic scanning microcalorimeter was obtained with funds provided by National Science Foundation equipment grant GP43396 to the Department of Chemistry, University of Oregon. This work was generously supported by National Institutes of Health grant GM15547 and NSF grant no GB29709 (to W.L.P.) and National Research Service Award (CA548801) from the National Cancer Institute (to B.P.G.).

Received for publication 26 May 1977 and in revised form 3 September 1977.

REFERENCES

1. GABER, B. P., and W. L. PETICOLAS. 1977. On the quantitative interpretation of biomembrane structure by Raman spectroscopy. *Biochim. Biophys. Acta.* **465**:260–274.
2. PRIVALOV, P. L., V. V. PLOTNIKOV, and V. V. FILIMONOV. 1975. Precision scanning microcalorimeter for the study of liquids. *J. Chem. Thermodynamics.* **7**:41–47.
3. CHAPMAN, D. 1975. Phase transitions and fluidity characteristics of lipids and cell membranes. *Q. Rev. Biophys.* **8**:185–235.
4. SAVITSKY, A., and M. J. E. GOLAY. 1964. Smoothing and differentiation of data by simplified least squares procedures. *Anal. Chem.* **36**:1627.
5. CHRISMAN, R., J. C. ENGLISH, and R. S. TOBIAS. 1976. A high sensitivity digital Raman difference spectrometer for studies on solutions of biological molecules with on-line computer control of data acquisition and reduction. *Appl. Spectrosc.* **30**:168–179.
6. BUNOW, M. R., and I. W. LEVIN. 1977. Comment on the carbon-hydrogen stretching region of vibrational Raman spectra of phospholipids. *Biochim. Biophys. Acta.* **487**:388–394.
7. LIPPERT, J. L., and W. L. PETICOLAS. 1971. Laser Raman investigation of the effect of cholesterol on conformational changes in dipalmitoyl lecithin multilayers. *Proc. Natl. Acad. Sci. U. S. A.* **68**:1572–1576.
8. LIPPERT, J. L., and W. L. PETICOLAS. 1972. Raman active vibrations in long-chain fatty acids and phospholipid sonicates. *Biochim. Biophys. Acta.* **282**:8–17.
9. MENDELSOHN, R., S. SUNDER, and H. J. BERNSTEIN. 1976. Structural studies of biological membranes and related model systems by Raman spectroscopy. Sphingomyelin and 1,2-dilauroylphosphatidylethanolamine. *Biochim. Biophys. Acta.* **413**:329–340.
10. LARSSON, K. 1973. Conformation-dependent features in the Raman spectra of simple lipids. *Chem. Phys. Lipids.* **10**:165.
11. BULKIN, B. J., and N. KRISHNAMACHARI. 1972. Vibrational spectra of liquid crystals. IV. Infrared and Raman spectra of phospholipid-water mixtures. *J. Am. Chem. Soc.* **95**:109.
12. BROWN, K. G., W. L. PETICOLAS, and E. BROWN. 1973. Raman studies of conformational changes in model membrane systems. *Biochem. Biophys. Res. Commun.* **54**:358–368.
13. YELLIN, N., and I. W. LEVIN. 1977. Hydrocarbon chain trans-gauche isomerization in phospholipid bilayer gel assemblies. *Biochemistry.* **16**:642–647.
14. BULKIN, B. 1976. Infrared and Raman spectroscopy of liquid crystals. *Appl. Spectrosc.* **30**:261–269.
15. LIS, L. J., S. C. GOHEEN, J. W. KRUFFMAN, and D. F. SHRIVER. 1976. Laser Raman spectroscopy of lipid protein systems. Differences in the effect of intrinsic and extrinsic protein on phosphatidylcholine Raman spectrum. *Biochim. Biophys. Acta.* **443**:331–338.
16. NAGLE, J. R. 1973. A theory of Biomembrane phase transitions. *J. Chem. Phys.* **58**:252–264.
17. SNYDER, R. G. 1967. Vibrational study of the chain conformation of the liquid η-paraffins and molten polyethylene. *J. Chem. Phys.* **47**:1316.
18. PETICOLAS, W. L., L. A. NAFIE, P. B. STEIN, and B. FANCONI. 1970. Quantum theory of the intensities of molecular vibrational spectra. *J. Chem. Phys.* **52**:1576–1584.
19. TATEVSKII, V. M., V. A. BENDERSKII, and S. S. YAROVOI. 1961. Rules and methods for calculating the physicochemical properties of paraffinic hydrocarbons. Pergamon Press, Inc., Elmsford, N.Y.
20. SNYDER, R. G., S. L. HSU, and S. KRIMM. 1978. Vibrational spectra in the C-H stretching region and the structure of the polymethylene chain. *Spectrochim. Acta.* In press.
21. JANIAK, M. J., D. M. SMALL, and G. G. SHIPLEY. 1976. Nature of the thermal pretransition of synthetic phospholipids: dimyristoyl- and dipalmitoyllecithin. *Biochemistry.* **15**:4575–4580.
22. LADBROOKE, B. D., and D. CHAPMAN. 1969. Thermal analysis of lipids, proteins and biological membranes: a review and summary of recent studies. *Chem. Phys. Lipids.* **3**:304–367.